Comparison of Data-driven Link Estimation Methods in Low-power Wireless Networks

Hongwei Zhang
Department of Computer Science
Wayne State University, USA
hzhang@cs.wayne.edu

Lifeng Sang, Anish Arora
Department of Computer Science and Engineering
The Ohio State University, USA
{sangl, anish}@cse.ohio-state.edu

Abstract—Link estimation is a basic element of routing in low-power wireless networks, and data-driven link estimation using unicast MAC feedback has been shown to outperform broadcast-beacon based link estimation. Nonetheless, little is known about the impact that different data-driven link estimation methods have on routing behaviors. To address this issue, we classify existing data-driven link estimation methods into two broad categories: *L-NT* that uses aggregate information about unicast and *L-ETX* that uses information about the individual unicast-physical transmissions. Through mathematical analysis and experimental measurement in a testbed of 98 XSM motes (an enhanced version of MICA2 motes), we examine the accuracy and stability of L-NT and L-ETX in estimating the ETX routing metric. We also experimentally study the routing performance of L-NT and L-ETX. We discover that these two representative, seemingly similar methods of data-driven link estimation differ significantly in routing behaviors: L-ETX is much more accurate and stable than L-NT in estimating the ETX metric, and, accordingly, L-ETX achieves a higher data delivery reliability and energy efficiency than L-NT (for instance, by 25.18% and a factor of 3.75 respectively in our testbed). These findings provide new insight into the subtle design issues in data-driven link estimation that significantly impact the reliability, stability, and efficiency of wireless routing, thus shedding light on how to design link estimation methods for mission-critical wireless networks which pose stringent requirements on reliability and predictability.

Index Terms—Low-power wireless networks, sensor networks, link estimation and routing, data-driven, beacon-based

I. INTRODUCTION

Wireless communication assumes complex spatial and temporal dynamics [1], [2], [3], [4], thus estimating link properties is a basic element of routing in wireless networks. One link estimation method that is commonly used in early wireless routing protocol design [5], [6] is letting neighbors exchange broadcast beacon packets, and then estimating link properties of unicast data transmissions via those of broadcast beacons. Nonetheless, unicast and broadcast differ in many ways such as transmission rate and MAC coordination method [7], [8], and it is difficult to precisely estimate unicast link properties via those of broadcast due to factors such as the impact that dynamic, unpredictable network traffic patterns have on link properties [9], [10].

The research community has become increasingly aware of the drawbacks of beacon-based link estimation, and has proposed and started to use data-driven link estimation methods where unicast MAC feedback serves as the basis of link estimation [11], [12], [13], [14], [15], [6], [10]. Even though data-driven link estimation has been shown to outperform broadcast-beacon based link estimation in routing [10], [11], [14], little is known about how different data-driven link estimation methods affect the reliability, latency, stability, and energy efficiency of routing. This is an important problem because, as low power wireless sensor networks are increasingly deployed for mission critical tasks such as industrial monitoring, it is critical to ensure high reliability, low latency, and high predictability in routing. Moreover, as the rich information carried in MAC feedback (e.g., both the number of physical transmissions and the time taken for a unicast transmission) are used in an increasingly broader context, it is important to understand the impact of the different ways of using these information.

To answer the aforementioned open questions, our objectives in this paper are to comparatively study the different methods of data-driven link estimation and to distill the guidelines of using MAC feedback information in wireless link estimation and routing. In most wireless MACs, a unicast packet is retransmitted, upon transmission failure, until the transmission succeeds or until the number of transmissions has reached a certain threshold value such as 8. For convenience, we call the individual transmissions involved in transmitting a unicast packet the *unicast-physical-transmission*s. Accordingly, we classify existing data-driven link estimation methods depending on whether they use the aggregate information about unicast or they use information about the individual unicast-physical transmissions. For the routing metric ETX (i.e., expected number of transmissions), more specifically, we find that existing data-driven link estimation methods can be represented by two seemingly similar protocols: *L-NT* where the number of physical transmissions for each unicast is directly used to estimate link ETX, and *L-ETX* where we use the number of physical transmissions for each unicast to calculate the reliability of individual unicast-physical-transmissions which is then used to estimate link ETX.

Through mathematical analysis and experimental measurement in a testbed of 98 XSM motes (an enhanced version of MICA2 motes), we examine the accuracy and stability of L-NT and L-ETX in estimating the ETX routing metric. Using traffic traces for both bursty event detection and periodic data collection and using both grid and random network topologies, we also experimentally study the routing performance of L-NT and L-ETX. We discover that these two representative, seemingly similar methods of data-driven link estimation differ significantly in routing behaviors. L-ETX is much more accurate and stable

than L-NT in estimating the ETX metric, and L-ETX correctly identifies the optimal routes with a higher probability than L-NT does. Accordingly, L-ETX achieves a higher data delivery reliability, higher energy efficiency, and higher throughput than L-NT (for instance, by 25.18%, a factor of 3.75, and a factor of 3.53 respectively in our testbed); L-ETX also uses longer yet more reliable links, thus introducing lower data delivery latency and latency jitter than L-NT. We also find that the higher stability in L-ETX enables a much higher stability in routing, thus improving the predictability of routing performance which is critical to mission-critical networked control. These findings provide new insight into the subtle design issues in data-driven link estimation that significantly impact the reliability, latency, and predictability of wireless routing, thus shedding light on the principles of using MAC feedback information in mission-critical wireless networks.

The rest of the paper is organized as follows. We compare different methods of using MAC feedback in Section II, and we present the impact of link estimation accuracy on routing behaviors in Section III. (*Due to the limitation of space, we relegate to [16] the discussions of additional performance evaluation results and protocols similar to L-NT and L-ETX.*) Finally, we discuss related work in Section IV and make concluding remarks in Section V.

II. METHODS OF DATA-DRIVEN ESTIMATION

In this section, we first identify the two representative methods (i.e., L-NT and L-ETX) of data-driven link estimation, then we comparatively study their estimation accuracy via mathematical and experimental analysis.

A. Different data-driven estimation methods

MAC feedback for a unicast transmission usually contains aggregate information (e.g., MAC latency, number of physical transmissions, and transmission status) about transmitting the unicast packet as a whole, but from these information we can derive properties of the individual physical transmissions involved in unicasting. Accordingly, we can classify existing data-driven link estimation methods depending on whether they directly use the aggregate information about unicast or they use information about the individual unicast-physical-transmissions. In the literature, SPEED [12], LOF [10], and CARP [14] use the aggregate information MAC-latency, yet protocols such as four-bit-estimation [11], EAR [13], NADV [15], and MintRoute[6] use the reliability information about individual unicast-physical-transmissions. In this paper, we mainly focus on the following two data-driven link estimation methods:

- L-NT: directly use feedback information on the *number of physical transmissions* (NT) to estimate the expected number of physical transmissions (ETX) required to successfully deliver a packet across a link;
- L-ETX: first use feedback information to estimate the reliability, denoted as PDR, of individual unicast-physical-transmissions, then estimate ETX as $\frac{1}{\text{PDR}}$.

More specifically, given the same time series of MAC feedback information on unicast transmissions along a link, L-NT and L-ETX try to estimate ETX_t and PDR_t respectively, where ETX_t

is the ETX for the link and PDR_t is the expected reliability of unicast-physical-transmissions along the link. In L-NT, the time series input $\{x_i : i = 1, 2, \ldots\}$ to its estimator is $\{\text{NT}_i : i = 1, 2, \ldots\}$, where NT_i is the number of physical transmissions taken to deliver the i-th unicast packet; in L-ETX, the time series input $\{x_i\}$ is $\{\text{PDR}_{i'} : i' = 1, 2, \ldots\}$, where $\text{PDR}_{i'}$ is the packet delivery rate of the i'-th window of unicast-physical-transmissions with window size W (i.e., the average delivery rate of the $((i'-1) \times W+1)$-th, $((i'-1) \times W+2)$-th, ..., and the $((i'-1) \times W+W)$-th unicast-physical-transmission). Note that, for the i-th unicast packet, NT_i is calculated based on MAC feedback on the number NT'_i of physical transmissions incurred and the status of the unicast transmission showing whether the packet has been successfully delivered or not. If the status shows success, then $\text{NT}_i = \text{NT}'_i$; otherwise, the feedback simply shows that the packet has not been delivered after transmitting NT'_i times, thus we set NT_i as $\frac{\text{NT}'_i}{P^u_i}$ ($0 < P^u_i < 1$), where P^u_i is the average unicast reliability calculated based on the status information on transmitting the i unicast packets so far.

The rationale for considering the two methods L-NT and L-ETX are as follows:

- ETX is a commonly used metric in wireless network routing;
- The parameter NT is tightly related to MAC latency (e.g., MAC latency is approximately proportional to NT given a certain degree of channel contention) such that L-NT also represents protocols that directly use MAC latency in routing; (*we show in [16] that MAC-latency based protocols perform similar to L-NT.*)
- L-NT and L-ETX estimate the same link property ETX, which enables fair comparison between different data-driven estimation methods.

Based on this research design, L-NT represents the method used in SPEED, LOF, and CARP, and L-ETX represents the method used in four-bit-estimation, EAR, NADV, and MintRoute.

In what follows, we first mathematically analyze the differences between L-NT and L-ETX to gain basic insight into the behaviors of different link estimation methods, then we experimentally measure the behaviors of L-NT and L-ETX to corroborate the analytical observations.

B. Analysis of L-NT and L-ETX

In low-power, resource constrained wireless sensor networks, most routing protocols use simple, light-weight estimators such as the exponentially-weighted-moving-average (EWMA) estimator and its variations. Therefore, our analysis in this section focuses on the accuracy of estimating ETX for a wireless link via the commonly-used EWMA estimator. But the analytical results also apply to variations of the basic EWMA estimator such as the Window-Mean-with-EWMA (WMEWMA) estimator [6] and the Flip-Flop Filter (FF) [17].

Given a time series $\{x_i : i = 1, 2, \ldots\}$ where x_i is a random variable with mean μ and variance σ^2, the corresponding EWMA estimator for μ is

$$
\begin{aligned}
y_1 &= x_1 \\
y_k &= \alpha y_{k-1} + (1-\alpha)x_k, \ 0 \le \alpha \le 1, \quad k = 2, 3, \ldots
\end{aligned}
$$

By induction, we have

$$y_k = \alpha^k x_1 + (1 - \alpha) \sum_{i=1}^{k} \alpha^{k-i} x_i, \quad k \geq 1$$

In what follows, we first analyze the accuracy of EWMA estimator in general, then we compare the accuracy of L-NT and L-ETX. For mathematical tractability, our analysis assumes that each unicast-physical-transmission is a Bernoulli trial with a failure probability P_0 ($0 \leq P_0 < 1$). We corroborate the validity of our analytical results through testbed-based experimental analysis in Sections II-C and III.

Accuracy of EWMA estimators. To measure the estimation error in the estimator $\hat{\mu} = y_k$, we define *squared error* (SE) as

$$
\begin{aligned}
SE_k &= (y_k - \mu)^2 \\
&= ((\alpha^k x_1 + (1-\alpha)\sum_{i=1}^{k}\alpha^{k-i}x_i) - \mu)^2 \\
&= (\alpha^k(x_1 - \mu) + (1-\alpha)\sum_{i=1}^{k}\alpha^{k-i}(x_i - \mu))^2 \\
&= \alpha^{2k}(x_1 - \mu)^2 + (1-\alpha)^2\sum_{i=1}^{k}\alpha^{2(k-i)}(x_i - \mu)^2 + \\
&\quad CP_k
\end{aligned}
\tag{1}
$$

where

$$
\begin{aligned}
CP_k &= (1-\alpha)\sum_{i=1}^{k}\alpha^{-i}(x_1 - \mu)(x_i - \mu) + \\
&\quad (1-\alpha)^2\sum_{i=1}^{k}\sum_{j\neq i, j=1}^{k}\alpha^{2k-i-j}(x_i - \mu)(x_j - \mu)
\end{aligned}
$$

Therefore, the *mean squared error* (MSE) is

$$
\begin{aligned}
MSE_k &= E[SE_k] \\
&= \alpha^{2k}E[(x_1 - \mu)^2] + \\
&\quad (1-\alpha)^2\sum_{i=1}^{k}\alpha^{2(k-i)}E[(x_i - \mu)^2] + \\
&\quad E[CP_k]
\end{aligned}
\tag{2}
$$

Note that the expectation $E[]$ is taken over $x_1, x_2, \ldots, x_k$.

When each unicast-physical-transmission is a Bernoulli trial, the x_i's are mutually uncorrelated in both L-NT and L-ETX, that is, $E[x_i x_j] = E[x_i]E[x_j]$ if $i \neq j$. Then for $i \neq j$,

$$
\begin{aligned}
E[(x_i - \mu)(x_j - \mu)] &= E[x_i x_j - x_i \mu - \mu x_j + \mu^2] \\
&= E[x_i]E[x_j] - \\
&\quad E[x_i]\mu - \mu E[x_j] + \mu^2 \\
&= 0
\end{aligned}
$$

Thus,

$$
\begin{aligned}
E[CP_k] &= (1-\alpha)\sum_{i=1}^{k}\alpha^{-i}E[(x_1 - \mu)(x_i - \mu)] + \\
&\quad (1-\alpha)^2 \times \\
&\quad \sum_{i=1}^{k}\sum_{j\neq i, j=1}^{k}\alpha^{2k-i-j}E[(x_i - \mu)(x_j - \mu)] \\
&= 0
\end{aligned}
\tag{3}
$$

From Equations 2 and 3, we have

$$
\begin{aligned}
MSE_k &= \alpha^{2k}\sigma^2 + (1-\alpha)^2\sum_{i=1}^{k}\alpha^{2(k-i)}\sigma^2 \\
&= \sigma^2\frac{2\alpha^{2k+1}-\alpha+1}{1+\alpha}
\end{aligned}
\tag{4}
$$

To measure the *degree of estimation error* (DE) using estimator $\hat{\mu} = y_k$, we define DE_k as $\frac{\sqrt{MSE_k}}{\mu}$. Thus

$$
\begin{aligned}
DE_k &= \frac{\sqrt{MSE_k}}{\mu} \\
&= \frac{\sigma}{\mu}\sqrt{\frac{2\alpha^{2k+1}-\alpha+1}{1+\alpha}} \\
&= COV[X]\sqrt{\frac{2\alpha^{2k+1}-\alpha+1}{1+\alpha}}
\end{aligned}
\tag{5}
$$

where $COV[X]$ is the coefficient-of-variation (COV) of the $x's$, i.e., $COV[X] = \frac{\sigma}{\mu}$. Therefore, we have

Proposition 1: Assuming that x_i and x_j ($i \neq j$) are uncorrelated, the degree of estimation error using EWMA estimator is proportional to the COV of the x's. □

Relative accuracy of L-NT and L-ETX. To compare the DEs of L-NT and L-ETX, therefore, we first analyze the COV of NT_i and $PDR_{i'}$ as follows:

- L-NT: By definition, NT_i can be modeled as following a geometric distribution with the probability of success $1 - P_0$. Thus $E[NT_i] = \frac{1}{1-P_0}$, and $std[NT_i] = \frac{\sqrt{1-(1-P_0)}}{1-P_0} = \frac{\sqrt{P_0}}{1-P_0}$. Therefore,

$$COV[NT_i] = \frac{std[NT_i]}{E[NT_i]} = \sqrt{P_0} \tag{6}$$

- L-ETX: Given a window size $W > 1$, the number N of successes in W physical transmissions can be modeled as following a Binomial distribution with the probability of success $1 - P_0$ and the number of trials W. Thus, $E[N] = W(1 - P_0)$, and $var[N] = W(1 - P_0)P_0$. Let $PDR_{i'} = \frac{N}{W}$, then $E[PDR_{i'}] = \frac{1}{W}E[N] = 1 - P_0$, $var[PDR_{i'}] = \frac{1}{W^2}var[N] = \frac{(1-P_0)P_0}{W}$, and $std[PDR_{i'}] = \sqrt{var[PDR_{i'}]} = \frac{\sqrt{(1-P_0)P_0}}{\sqrt{W}}$. Therefore,

$$COV[PDR_{i'}] = \frac{std[PDR_{i'}]}{E[PDR_{i'}]} = \frac{\sqrt{P_0}}{\sqrt{W(1-P_0)}} \tag{7}$$

From Equations (6) and (7), we see that

$$COV[NT_i] > COV[PDR_{i'}], \text{ if } W > \frac{1}{1-P_0} \tag{8}$$

Note that the condition $W > \frac{1}{1-P_0}$ generally holds in practical scenarios, since W is generally greater than 2 and P_0 is generally less than 50% [18], [10].

From Proposition 1 and Inequality (8), then we have

Proposition 2: Given an EWMA estimator and assuming that each unicast-physical-transmission is a Bernoulli trial, $DE_k(\text{L-ETX}) < DE_k(\text{L-NT})$ if $W > \frac{1}{1-P_0}$; that is, L-ETX is more accurate than L-NT in estimating the ETX value of a link as long as $W > \frac{1}{1-P_0}$. □

Proof sketch: We first show that $DE(\text{L-ETX}) \approx DE(\text{PDR})$ as follows. Let P_t be the actual $E[PDR]$, ETX_t be the actual ETX and equal to $\frac{1}{P_t}$, and P_e be the estimated $E[PDR]$. Then the absolute estimation error ΔETX of ETX is as follows:

$$\Delta\text{ETX} = |\frac{1}{P_e} - \frac{1}{P_t}| = \frac{1}{P_t}|\frac{P_t - P_e}{P_e}| = ETX_t\frac{|P_t - P_e|}{P_e}$$

Thus

$$DE(\text{L-ETX}) = \frac{E[\Delta\text{ETX}]}{ETX_t} = E[\frac{|P_t - P_e|}{P_e}] \approx DE[\text{PDR}].$$

In the mean time, we know from Proposition 1 and Inequality 8 that $DE_k(\text{L-NT}) > DE_k[\text{PDR}]$. Therefore, $DE_k(\text{L-NT}) > DE_k(\text{L-ETX})$.

□

From the above analysis, we see that, even though L-NT and L-ETX use the same MAC feedback information in a seemingly similar fashion (e.g., $PDR_{i'}$'s assume, approximately, a form of the reciprocal of NT_i's), the variability (more precisely, the COV) of NT_i's tends to be greater than that of $PDR_{i'}$'s, and this difference in variability makes L-NT a less accurate estimator than L-ETX. We corroborate these analytical observations through experimental analysis in Sections II-C and III.

Impact of W and α. Note that, even though they do not affect the relative accuracy of L-NT and L-ETX, the window size W used in L-ETX and the weight factor α of the EWMA estimator also affect estimation accuracy. In what follows, we briefly discuss the impact of W and α.

From Equations 5 and 7, we see that larger window size W will lead to smaller estimation error in L-ETX; on the other hand, a larger W leads to reduced agility for the estimator to respond to changes, which can negatively affect routing performance in the presence of network dynamics. In practice, we usually choose a medium-sized W as a tradeoff between estimation accuracy and agility, and W is set as 20 for the study of this paper.

Let $Q_k(\alpha) = \sqrt{\frac{2\alpha^{2k+1} - \alpha + 1}{1+\alpha}}$, then, by Equation 5, DE_k is proportional to $Q_k(\alpha)$. Figure 1 shows the impact of α on

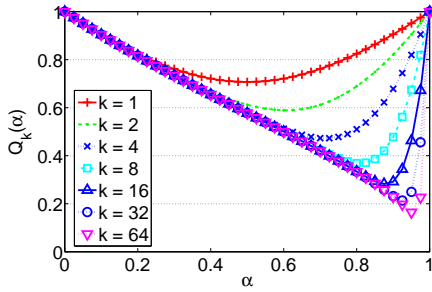
Fig. 1. $Q_k(\alpha)$

$Q_k(\alpha)$ and thus DE_k. We see that the optimal α value increases as k increases, and the intuition is that, as k increases, the contribution of the history data (i.e., $x_0, x_1, \ldots, x_{k-1}$) to y_k becomes more and more important compared with that of the most recent observation x_k. On the other hand, the agility of the estimator decreases as α increases. After α exceeds certain threshold value, moreover, $Q_k(\alpha)$ (and thus DE_k) increases as α increases further. In practice, therefore, we can choose a value that tradeoffs between estimation precision and agility, and we set α as $\frac{7}{8}$ in our study.

C. Experimentation with L-NT and L-ETX

Having shown that L-ETX is a more accurate estimation method than L-NT in Proposition 2, we experimentally evaluate the validity of the analytical results and study the impact of estimation accuracy on the optimality and stability of routing using the *Kansei* [19] sensor network testbed. In what follows, we first present the experiment design and then the experimental results.

Experiment design. In an open warehouse with flat aluminum walls (see Figure 2(a)), Kansei deploys 98 XSM motes [20] in a 14×7 grid (see Figure 2(b)) where the separation between neighboring grid points is 0.91 meter (i.e., 3 feet). The grid

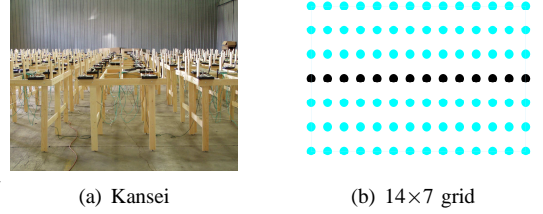(a) Kansei   (b) 14×7 grid

Fig. 2. Sensor network testbed *Kansei*

deployment pattern enables experimentation with regular, grid topologies, as well as random topologies (e.g., by randomly selecting nodes of the grid to participate in experiments). XSM is an enhanced version of Mica2 mote, and each XSM is equipped with a Chipcon CC1000 radio operating at 433 MHz. To form multihop networks, the transmission power of the CC1000 radios is set at -14dBm (i.e., power level 3) for the experiments of this paper unless otherwise stated. XSM uses TinyOS [21] as its operating system. For all the experiments in this paper, the default TinyOS MAC protocol B-MAC [22] is used; a unicast packet is retransmitted, upon transmission failure, at the MAC layer (more specifically, the TinyOS component QueuedSend) for up to 7 times until the transmission succeeds or until the 8 transmissions have all failed; a broadcast packet is transmitted only once at the MAC layer (without retransmission even if the transmission has failed).

To collect measurement data on unicast link properties, we let the mote on the left end of the middle row (shown as black dots in Figure 2(b)) be the *sender* and the rest 13 motes of the middle row as the *receiver*s, and we measure the unicast properties of the links between the sender and individual receivers. (Note that we have observed similar phenomena as what we will present in this section for other sender-receiver pairs.) The sender transmits 15,000 unicast packets to each of the receivers with a 128-millisecond inter-packet interval, and each packet has a data payload of 30 bytes. Based on packet reception status (i.e., success or failure) at the receivers, we measure unicast link properties.

To examine the impact of traffic-induced interference on link properties and link estimation, we randomly select 42 motes out of the light-colored (of color cyan) 6 rows as *interferer*s, with 7 interferers from each row on average. Each interferer transmits unicast packets (of payload length 30 bytes) to a destination randomly selected out of the other 41 interferers. The load of the interfering traffic is controlled by letting interferers transmit packets with a certain probability d whenever the channel becomes clear. Ng *et al.* [23] showed that the optimal traffic injection rate is 0.245 in a regular linear topology, and the optimal traffic injection rate will be even lower in general, two-dimensional network. Thus our measurement study focuses more on smaller d's than on larger ones, but we still study larger d's to get a sense on how systems behave in extreme conditions.

More specifically, we use the following d's in our study: 0, 0.01, 0.04, 0.07, 0.1, 0.4, 0.7, and 1. Thus the interference pattern is controlled by d in this case. (Note that phenomena similar to what we will present have been observed for other interfering traffic patterns, for instance, with different spatial distribution and different number of interferers.) We have done the experimental analysis for different d's and observed similar phenomena. Due to the limitation of space, here we only present data for the case when $d = 0.1$.

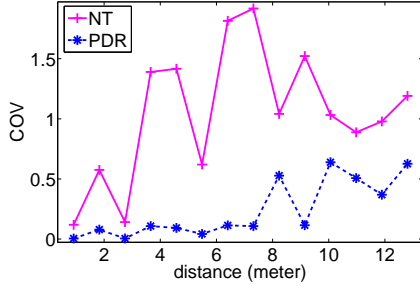**Estimation accuracy.** Figure 3 shows the COV of NT and PDR

Fig. 3. COV[NT] vs. COV[PDR] when $d = 0.1$; Note that the reason why the COVs are not monotonic with link length (i.e., sender-receiver distance) is because of radio and environment variations [4]. In this paper, we use distance mainly to identify individual links associated with a sender, and for clarity of presentation, we do not present confidence intervals unless they are necessary for certain claims of the paper.

for different links. We see that COV[NT] is significantly greater, up to a factor of 17.78, than COV[PDR], which is consistent with our analysis as shown by Inequality 8. Accordingly, the degree of estimation error (DE) in L-NT is consistently greater than that in L-ETX, as shown in Figure 4 where DE(L-NT)
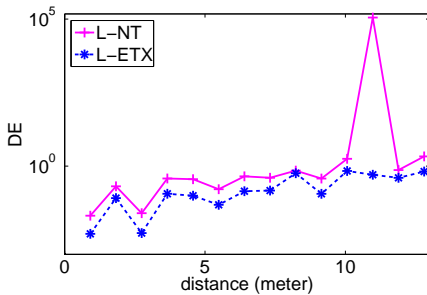
Fig. 4. DE(L-NT) vs. DE(L-ETX) when $d = 0.1$

and DE(L-ETX) for different links are presented. Therefore, the experimental results corroborate the prediction of Proposition 2. Note that the reason why, given an estimation method, the trend for its curves of COV and DE are slightly different (unlike what Equation 5 would suggest to be exactly the same) is due to the simplifying assumption (i.e., each unicast-physical-transmission is a Bernoulli trial) used in the analysis. Nonetheless, the analytical and experimental analysis do agree on the relative accuracy between L-NT and L-ETX. The reason why the DE value for the 11-meter-long link is very large in L-NT is due to the extremely low reliability of the link and the fact, as we

show immediately below, that L-NT introduces large estimation errors in the presence of transmission failures.

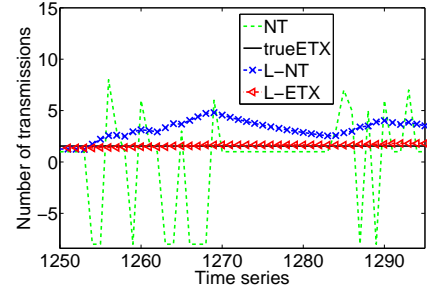To elaborate on the details of link estimation, Figure 5 shows,

Fig. 5. Time series of estimated ETX values in L-NT and L-ETX for a link of length 9.15 meters (i.e., 30 feet)

for a link of length 9.15 meters (i.e., 30 feet), the time series of the estimated ETX values via L-NT and L-ETX respectively. (Note: the figure is more readable in color-print than black-white print.) To visualize the accuracy of L-NT and L-ETX, we also show the NT values carried in MAC feedbacks and the actual ETX value for the link. To easily represent a unicast transmission failure (after 7 retransmissions), we present -8 as the NT value for the corresponding unicast transmission. We see that the estimated ETX in L-NT tends to deviate from the actual ETX value, especially in the presence of MAC transmission failures; the estimated ETX in L-ETX, however, is very close to the actual ETX value, even in the presence of MAC transmission failures. We also see that the estimated ETX value in L-ETX is pretty stable whereas the estimation of L-NT oscillates significantly, which has significant implications to routing behaviors as we discuss next and in Section III-B.

Routing optimality and stability. To understand the routing behaviors in L-NT and L-ETX, we consider the case where the sender on the left end of the middle row of Figure 2(b) needs to select the best next-hop forwarder among the set of receivers in the middle row, and the destination is far away from the sender but in the direction extending from the sender along the middle row to the right. For simplicity, we assume that the sender uses a localized, geographic routing metric ETD (for *ETX per unit-distance to destination*) in evaluating the goodness of forwarder candidates. The metric ETD is defined as follows: given a sender S, a neighbor R of S, and the destination D, the ETD via R is defined as

$$
\begin{cases}
\frac{ETX_{S,R}}{L_{S,D} - L_{R,D}} & \text{if } L_{S,D} > L_{R,D} \\
\infty & \text{otherwise}
\end{cases}
\tag{9}
$$

where $ETX_{S,R}$ is the ETX of the link from S to R, $L_{S,D}$ denotes the distance from S to D, and $L_{R,D}$ denotes the distance from R to D. (*We show in [16] that this local, geographic metric performs in a similar way as the global, distance-vector metric for uniformly distributed networks.*)

In our case, the best forwarder is 10 grid-hops away from the sender since the corresponding link has the minimum ETD value. To see how L-NT and L-EXT perform in selecting the

Method	Forwarder	Percentage (%)	Cost ratio
L-NT	5	0.1	2.3
	6	4.14	1.3
	7	7.17	1.5
	8	21.26	1.3
	10	67.33	1
L-ETX	6	5.91	1.3
	7	0.2	1.5
	8	5.1	1.3
	10	88.79	1

TABLE I
FORWARDERS USED IN L-NT AND L-ETX

next-hop forwarder, Table I shows the forwarders (identified in terms of their grid hop distance from the sender) used in L-NT and L-ETX respectively. To illustrate the optimality of different methods, we measure the percentage of time each forwarder is used, and the cost ratio of this forwarder to the optimal forwarder 10. We see that L-ETX is able to identify and use the optimal forwarder more than 20% of the time compared with L-NT. The average ETD of using L-ETX is 3.26% more than the optimal ETD, yet the average ETD of using L-NT is 11.34% more than the optimal ETD.

We also measure the number of times that the sender changes its forwarder when using L-NT and L-ETX respectively, and we observe that the number of forwarder changes is 95 and 13 in L-NT and L-ETX respectively. Thus, L-ETX ensures much higher routing stability than L-NT, which is due to the fact that L-ETX is a more stable estimator than L-NT as can be seen from Figure 5. Higher routing stability helps improve the predictability of packet delivery performance in networks.

III. ROUTING PERFORMANCE

Having discussed the significant impact that link estimation methods have on estimation accuracy and routing optimality in Section II, we experimentally evaluate the performance of different data-driven link estimation methods in this section. We first present the methodology and then compare different data-driven estimation methods.

A. Methodology

We use a publicly available event traffic trace for a field sensor network deployment [24] to evaluate the performance of different protocols. Since the traffic trace is collected from 49 nodes that are deployed in a 7×7 grid, we randomly select and use a 7×7 subgrid of the Kansei testbed (as shown in Figure 2(b)) in our experiments. To form a multi-hop network, we set the radio transmission power at -14dBm (i.e., power level 3). The mote at one corner of the subgrid serves as the base station, the other 48 motes generate data packets according to the aforementioned event traffic trace, and the destination of all the data packets is the base station. *We have also evaluated protocols with other traffic patterns, e.g., periodic data traffic, and other network setups, e.g., random networks. We have observed phenomena similar to what we will present, but we relegate the detailed discussion to [16] due to the limitation of space.*

Using the above setup, we comparatively study the performance of the following data-driven link estimation and routing protocols:[1]

- *L-NT*: a distance-vector routing protocol whose objective is to minimize the expected number of transmissions (ETX) from each source node to its destination. The ETX metric of each link (and thus each route) is estimated via the L-NT data-driven method.
- *L-ETX*: same as L-NT except that the ETX metric is estimated via the L-ETX method.
- *L-WNT*: a variant of L-NT where the input to the EWMA estimator is the average of 5 *NT* values for every 5 consecutive unicast transmissions. We study this protocol to check whether the performance of protocol L-NT can be improved by increasing the stability of the L-NT method through the window-based NT average.
- *L-NADV*: a variant of L-ETX where the window size W is 1 and the EWMA estimator is used to estimate packet error rate (PER) instead of PDR. We study this protocol mainly to examine the impact of W.[2] L-NADV is also the distance-vector version of the geographic protocol NADV [15].

In the above data-driven protocols, periodic, broadcast beacons are never used. We use the approach of *initial link sampling* [10] to jump-start the routing process, where a node proactively takes 7 samples of MAC feedback (by transmitting 7 unicast packets) for each of its candidate forwarders and then chooses the best forwarder based on the initial sampling results.

For each protocol we study, we ran the event traffic trace sequentially for 40 times, and we measure the following protocol performance metrics:

- *Event reliability (ER)*: the number of unique packets received at the base station divided by the total number of unique packets generated for an event. This metric reflects the amount of useful information that can be delivered for an event.
- *Number of transmissions per packet delivered (NumTx)*: the total number of physical transmissions incurred in delivering packets of an event divided by the number of unique packets received at the base station. This metric affects network throughput; it also reflects the energy efficiency of a protocol, since it not only affects the energy spent in transmission but also the degree of duty cycling which in turn affects the energy spent at the receiver side.

We also compare data delivery latency and predictability using our data on the reliability and detailed properties of the routes used in different protocols.

B. Experimental results

Figures 6 and 7 show the event reliability and the average number of transmissions required for delivering each packet in different data-driven protocols respectively, Figures 8 and

---

[1]In this paper, we sometimes use the same name for the protocol, the estimation method, and the routing metric. The context of its usage will clarify its exact meaning.

[2]Our experiments show that routing performance is statistically the same whether we use PER or PDR as the input to the EWMA estimator.
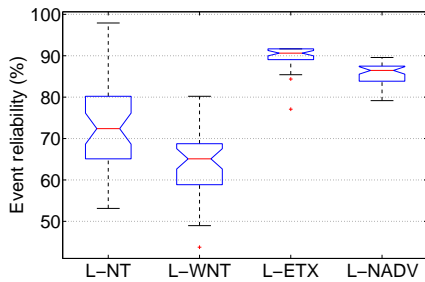
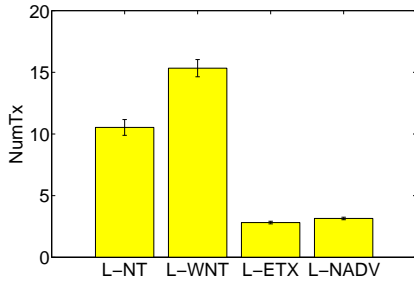Fig. 6. Event reliability

Fig. 7. Average number of transmissions per packet delivered, with the error bar representing the confidence intervals at the 95% confidence level

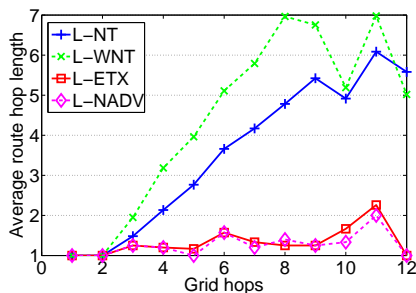9 show the average route hop length and route transmission

Fig. 8. Average route hop length for nodes different grid-hops away from the base station
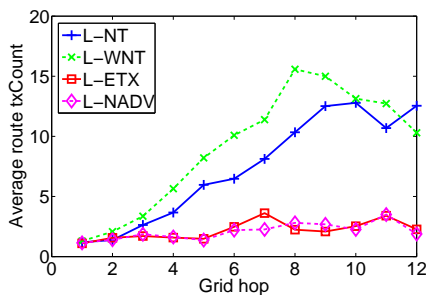

Fig. 9. Average route transmission count for nodes different grid-hops away from the base station

count respectively for successfully delivered packets coming

from nodes at different grid-hops away from the base station, and Table II shows the detailed information about the properties

Metric	L-NT	L-WNT	L-ETX	L-NADV
Average per-hop geo-distance (meter)	2.89	2.51	4.17	4.37
Average per-hop physical tx reliability (%)	56.3	51.08	68.43	66.77
Average per-hop unicast reliability (%)	87.62	87.02	93.10	89.21
Per-hop ETX	2.56	2.65	1.94	2.18

TABLE II
PER-HOP PROPERTIES IN DIFFERENT ROUTING PROTOCOLS

of the links used in different protocols.

L-NT vs. L-ETX. From Figure 6, we see that L-ETX achieves a significantly higher event reliability than L-NT. For instance, the median event reliability in L-ETX is 90.63%, which is 25.18% higher than that in L-NT. The higher event reliability in L-ETX is due to the facts that the routes used in L-ETX are shorter than those in L-NT and the reliability of the links used in L-ETX is higher than that in L-NT, as shown in Figure 8 and Table II respectively. Due to the same reason, L-ETX achieves significantly higher energy efficiency than L-NT, as shown in Figure 7. For instance, the average number of packet transmissions required in delivering a packet to the base station in L-ETX is 2.82, which is 3.75 times less than that in L-NT.

From Table II, we see that the links used in L-ETX are longer yet more reliable than those in L-NT. This implies that L-ETX enables nodes to choose better routes in forwarding data and thus leads to significantly better performance in data delivery.

The facts that L-ETX uses shorter-hop-length routes and that the links used in L-ETX are longer yet more reliable than those in L-NT also suggest that, for the same requirement on end-to-end data delivery reliability, the latency and latency jitter in data delivery are smaller in L-ETX than in L-NT. Higher reliability also implies less variability and better predictability in data delivery performance (e.g., latency), because, given a link reliability p, the variability (more precisely, coefficient-of-variation) of packet transmission status (i.e., success or failure) is $\sqrt{\frac{1-p}{p}}$ and it decreases as p increases. For instance, the standard deviation of the route transmission counts (and thus the delivery latency) for successfully delivered packets in L-ETX tends to be less than that in L-NT as shown in Figure 10. Therefore, compared with L-NT, L-ETX achieves a higher degree of predictability in routing performance, which is important for mission-critical networked sensing and control.

Variants of L-NT and L-ETX. Counterintuitively, Figures 6 and 7 show that L-WNT performs worse than L-NT, and Table II shows that L-WNT chooses worse routes than L-NT does. Through careful analysis, we find out that the cause for the worse performance of L-WNT is that, even though L-WNT is a more stable estimator than L-NT, it is slower (i.e., less agile) in adapting to link property changes. The slow convergence in L-WNT further exacerbates the error in NT-based estimation and leads to larger estimation error compared with L-NT, especially
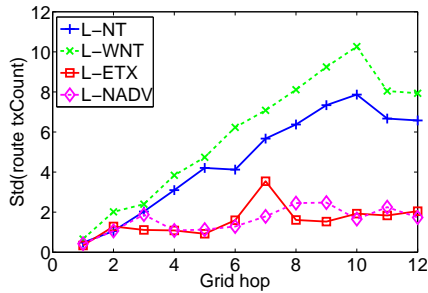
Fig. 10. Standard deviation of the route transmission count for nodes different grid-hops away from the base station

Two consecutive routes (%)	L-NT	L-WNT	L-ETX	L-NADV
Same	36.55	42	99.94	99.97
Diff. routes but same hop length	17.08	11.18	0.03	0.03
Increased hop length	23.96	24.19	0.03	0
Decreased hop length	22.41	22.63	0	0

TABLE III
ROUTE STABILITY MEASURED BY COMPARING THE ROUTES TAKEN BY EVERY TWO CONSECUTIVE PACKETS

in the presence of dynamics. This can be seen from Figure 11 which shows the time series of the estimated ETX values in L-
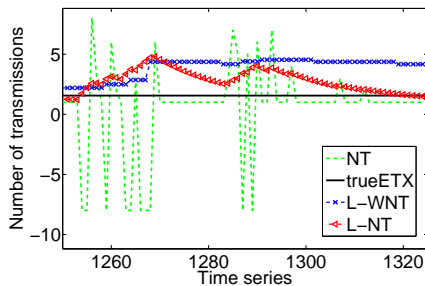

Fig. 11. Time series of estimated L-WNT and L-NT for a link of length 9.15 meters (i.e., 30 feet)

WNT and L-NT for a link of length 9.15 meters (i.e., 30 feet).

As expected, L-NADV performs slightly worse than L-ETX, as shown in Figure 6, Figure 7, and Table II. This is due to the larger estimation errors in L-NADV, especially in the presence of transmission failures. This can be seen from Figure 12 which
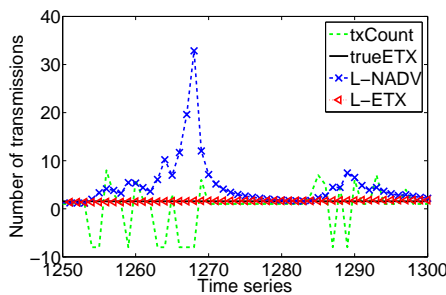

Fig. 12. Time series of estimated L-NADV and L-ETX for a link of length 9.15 meters (i.e., 30 feet)

presents the time series of the estimated ETX values in L-NADV and L-ETX for a link of length 9.15 meters (i.e., 30 feet).

Route stability. Table III shows the route stability measured by comparing the routes taken by every two consecutive packets. We see that L-ETX (and its variant L-NADV) is very stable and seldom changes route (only at a probability of ∼0.03%), yet L-NT (and its variant L-WNT) tends to be much more unstable.

The fact that nodes seldom change routes in L-ETX also shows that initial link sampling is able to identify the best forwarders for most nodes in L-ETX. High stability in routing not only helps facilitate other control logics such as QoS-oriented structuring and scheduling, it also improves the predictability of routing performance, which is important for mission-critical networked sensing and control. Detailed study of these is a part of our future work.

IV. RELATED WORK

Differences between broadcast and unicast and their impact on the performance of AODV were first discussed in [7] and [8], and the authors discussed reliability-based mechanisms (e.g., those based on RSSI or SNR) for blacklisting bad links. The authors also proposed mechanisms, such as enforcing SNR threshold on control packets, to ameliorate the negative impact of the differences, and the authors of [7] studied the impact of packet size, packet rate, and link reliability threshold on the end-to-end delivery rate in AODV. Nonetheless, the proposed solutions were still based on beacon exchanges among neighbors.

Zhang *et al.* systematically studied the inherent drawbacks of beacon-based link estimation and proposed to use unicast MAC feedback as the basis of link estimation in IEEE 802.11b and mote networks [10], [18]. Methods of using both MAC feedback and beacon packets in link estimation were also proposed in MintRoute [6], EAR [13], and four-bit-estimation [11]; SPEED [12], NADV [15], and CARP [14] also used MAC feedback in link estimation and route selection. Nonetheless, there has been no systematic study on the impact that the different ways of using MAC feedback have on routing behaviors, and our study in this paper fills this vacuum and provides insight into the principles of using MAC feedback in data-driven link estimation and routing.

Other routing metrics and protocols [25], [26], [27], [28], [29], [30], [31] have also been proposed for various optimization objectives (e.g., energy efficiency). The findings of this paper can be applied to these schemes to help improve the accuracy of estimating link and path properties. Directed diffusion [32] provides a framework for routing in sensor networks, and the findings of this paper can also be applied to this framework to help select high-performance routes in data forwarding.

Rather than selecting the next-hop forwarder before data transmission, opportunistic routing protocols that take advantage of spatial diversity in wireless transmission have been proposed

[33], [34], [35], [36]. In these protocols, the forwarder is selected, through coordination among receivers, in a reactive manner after data transmission. Link estimation can still be helpful in these protocols since it can help effectively select the best set of listeners [33]. Therefore, findings of this paper can be useful in opportunistic routing too.

Draves *et al.* comparatively studied several routing metrics in the context of beacon-based link estimation and routing [37], and they have found out that ETX is an effective metric for routing in mostly static wireless networks. Our work in this paper focuses on the different methods of using unicast MAC feedback to estimate the metric ETX, and we have demonstrated the importance of choosing the right method among seemingly similar approaches.

V. Concluding remarks

Through mathematical analysis and measurement based study, we have examined the impacts that different data-driven link estimation methods have on routing behaviors. We have shown that the variability of parameters being estimated significantly affects the reliability, latency, energy efficiency, and predictability of data-driven link estimation and routing, and it should be an important criterion to consider when choosing the data-driven link estimation method. We have shown that L-ETX is a precise, stable method of estimating the ETX of data transmissions, and that a seemingly similar method L-NT performs much worse in terms of packet delivery reliability, energy efficiency, and routing stability. These findings elucidate the subtleties of data-driven link estimation and provide guidelines on how to effectively use MAC feedback in link estimation.

The experimental analysis of this paper is based on networks of CC1000 radios. Even though we expect the findings of this paper to be valid for networks of IEEE 802.15.4 radios, systematic evaluation of this conjecture is a part of our future work. We have focused on accurate estimation of the ETX routing metric in this paper, identifying accurate estimation methods for other routing metrics such as mETX [27] and CTT [31] is also an important task to pursue for supporting different optimization objectives in routing.

References

[1] D. Aguayo, J. Bicket, S. Biswas, G. Judd, and R. Morris, "Link-level measurements from an 802.11b mesh network," in *ACM SIGCOMM*, 2004.

[2] D. Kotz, C. Newport, and C. Elliott, "The mistaken axioms of wireless-network research," Dartmouth College, Computer Science, Tech. Rep. TR2003-467, July 2003.

[3] J. Zhao and R. Govindan, "Understanding packet delivery performance in dense wireless sensor networks," in *ACM SenSys*, 2003.

[4] M. Zuniga and B. Krishnamachari, "An analysis of unreliability and asymmetry in low-power wireless links," *ACM Transactions on Sensor Networks*, vol. 3, no. 2, 2007.

[5] D. S. J. D. Couto, D. Aguayo, J. Bicket, and R. Morris, "A high-throughput path metric for multi-hop wireless routing," in *ACM MobiCom*, 2003.

[6] A. Woo, T. Tong, and D. Culler, "Taming the underlying challenges of reliable multihop routing in sensor networks," in *ACM SENSYS*, 2003.

[7] I. Chakeres and E. Belding-Royer, "The utility of hello messages for determining link connectivity," in *WPMC*, 2002.

[8] H. Lundgren, E. Nordstrom, and C. Tschudin, "Coping with communication gray zones in ieee 802.11b based ad hoc networks," in *ACM WoWMoM*, 2002.

[9] A. Willig, "A new class of packet- and bit-level models for wireless channels," in *IEEE PIMRC*, 2002.

[10] H. Zhang, A. Arora, and P. Sinha, "Link estimation and routing in sensor network backbones: Beacon-based or data-driven?" *IEEE Transactions on Mobile Computing*, May 2009.

[11] R. Fonseca, O. Gnawali, K. Jamieson, and P. Levis, "Four-bit wireless link estimation," in *ACM HotNets*, 2007.

[12] T. He, J. Stankovic, C. Lu, and T. Abdelzaher, "SPEED: A stateless protocol for real-time communication in sensor networks," in *IEEE ICDCS*, 2003.

[13] K.-H. Kim and K. G. Shin, "On accurate measurement of link quality in multi-hop wireless mesh networks," in *ACM MobiCom*, 2006.

[14] R. Krishnan, A. Raniwala, and T. cker Chiueh, "Design of a channel characteristics-aware routing protocol," in *IEEE INFOCOM miniconference*, 2008.

[15] S. Lee, B. Bhattacharjee, and S. Banerjee, "Efficient geographic routing in multihop wireless networks," in *ACM MobiHoc*, 2005.

[16] H. Zhang, L. Sang, and A. Arora, "Comparison of data-driven link estimation methods in low-power wireless networks," Wayne State University (http://www.cs.wayne.edu/∼hzhang/group/TR/DNC-TR-08-05.pdf), Tech. Rep., 2008.

[17] M. Kim and B. Noble, "Mobile network estimation," in *ACM MobiCom*, 2001.

[18] H. Zhang, L. Sang, and A. Arora, "Link estimation in lower power wireless networks: Beacon-based or data-driven?" Wayne State University (http://www.cs.wayne.edu/∼hzhang/group/TR/DNC-TR-08-06.pdf), Tech. Rep., 2008.

[19] E. Ertin, A. Arora, R. Ramnath, M. Nesterenko, V. Naik, S. Bapat, V. Kulathumani, M. Sridharan, H. Zhang, and H. Cao, "Kansei: A testbed for sensing at scale," in *IEEE/ACM IPSN/SPOTS*, 2006.

[20] P. Dutta, M. Grimmer, A. Arora, S. Bibyk, and D. Culler, "Design of a wireless sensor network platform for detecting rare, random, and ephemeral events," in *IEEE/ACM IPSN/SPOTS*, 2005.

[21] "TinyOS," http://www.tinyos.net/.

[22] J. Polastre, J. Hill, and D. Culler, "Versatile low power media access for wireless sensor networks," in *ACM SenSys*, 2004.

[23] P. C. Ng and S. C. Liew, "Throughput analysis of IEEE 802.11 multi-hop ad hoc networks," *IEEE/ACM Transactions on Networking*, vol. 15, no. 2, 2007.

[24] "An event traffic trace for sensor networks," http://www.cs.wayne.edu/∼hzhang/group/publications/Lites-trace.txt.

[25] Q. Cao, T. He, L. Fang, T. Abdelzaher, J. Stankovic, and S. Son, "Efficiency centric communication model for wireless sensor networks," in *IEEE INFOCOM*, 2006.

[26] Y. Gu and T. He, "Data forwarding in extremely low duty-cycle sensor networks with unreliable communication links," in *ACM SenSys*, 2007.

[27] C. E. Koksal and H. Balakrishnan, "Quality-aware routing metrics for time-varying wireless mesh networks," *IEEE JSAC*, vol. 24, no. 11, 2006.

[28] J. C. Park and S. K. Kasera, "Expected data rate: An accurate high-throughput path metric for multi-hop wireless routing," in *IEEE SECON*, 2005.

[29] D. Pompili, T. Melodia, and I. F. Akyildiz, "Routing algorithms for delay-insensitive and delay-sensitive applications in underwater sensor networks," in *ACM MobiCom*, 2006.

[30] M. Wachs, J. I. Choi, J. W. Lee, K. Srinivasan, Z. Chen, M. Jain, and P. Levis, "Visibility: A new metric for protocol design," in *ACM SenSys*, 2007.

[31] H. Zhai and Y. Fang, "Impact of routing metrics on path capacity in multirate and multihop wireless ad hoc networks," in *IEEE ICNP*, 2006.

[32] C. Intanagonwiwat, R. Govindan, and D. Estrin, "Directed diffusion: A scalable and robust communication paradigm for sensor networks," in *ACM MobiCom*, 2000.

[33] S. Biswas and R. Morris, "ExOR: Opportunistic multi-hop routing for wireless networks," in *ACM SIGCOMM*, 2005.

[34] S. Chachulski, M. Jennings, S. Katti, and D. Katabi, "Trading structure for randomness in wireless opportunistic routing," in *ACM SIGCOMM*, 2007.

[35] T. He, B. M. Blum, Q. Cao, J. A. Stankovic, S. H. Son, and T. F. Abdelzaher, "Robust and timely communication over highly dynamic sensor networks," *Real-Time Systems Journal*, vol. 37, 2007.

[36] F. Ye, G. Zhong, S. Lu, and L. Zhang, "GRAdient Broadcast: A robust data delivery protocol for large scale sensor networks," in *IEEE IPSN*, 2003.

[37] R. Draves, J. Padhye, and B. Zill, "Comparison of routing metrics for static multi-hop wireless networks," in *ACM SIGCOMM*, 2004.